



**“BABEȘ – BOLYAI” UNIVERSITY OF  
CLUJ – NAPOCA  
FACULTY OF PHYSICS**



**PhD Thesis Summary**

**„The physical properties studies of some half – metallic  
compounds”**

*Scientific Advisor*

**Prof.Dr. Romulus Tetean**

*Ph.D. Student*

**Grasin Robert O.**

**Keywords:** RE doped Heusler and half – Heusler alloys; X-ray diffraction; Analytical Electron Microscopy; Electronic band structure; Magnetic measurements; XPS spectra.

**Cluj – Napoca**

**2012**

## Introduction

In the last 30 years, a huge interest on the development of spintronic (see below) devices emerged because of their potential application to the next generation of electronic devices. In classic electronic devices, the charge of the electron is the carrier of the information. A big step in the field, was the discovery of ferromagnetic half – metals in which the *spin* of the electron takes the role of the information carrier. This emerges as a direct consequence of the existence of a gap at the Fermi level for one orientation of the electron spins. Theoretically the spin polarization of these half – metals is 100%, but because of experimental limits, samples usually have  $\sim 30 \div 45\%$  spin polarization. The so – called Heusler alloys have the highest potential in the development of materials with applications in spintronics. Band structure calculations confirmed that, because of the coupling between the magnetic moments of the transition metal (TM) *3d* itinerant electron spin and the rare earth (RE) *4f* electron spins, a gap in the conduction band for one of the spin orientations, will appear.

The goal of our work was to identify and prepare new half – metallic compounds with a high degree of spin polarization. Cummulative efforts in this research area will surely lead to the development of new materials with desired physical properties, with a big impact on the industry of electronic devices

This PhD thesis summarizes our results. In Chapter A, a general introduction on “Heusler alloys”, together with their structural and magnetic properties is presented. The experimental set – ups employed for the sample preparation and the characterization of their physical properties is presented in Chapter B. The following two chapters, C and D, include our results on RE doped Heusler and half – Heusler alloys, namely:  $\text{Co}_2\text{Mn}_{1-x}\text{RE}_x\text{Si}$  in Chapter C,  $\text{NiMn}_{1-x}\text{RE}_x\text{Sb}$  in Chapter D. The conclusions on each group of materials are summarized at the end of the corresponding chapter. At the end of the thesis you will find the general conclusions followed by the list of articles, figures and tables.

## A. Heusler alloys

Half – metallic ferromagnets (HFM) are a new class of materials with interesting physical properties. Half – metallicity was predicted in 1983 by De Groot [Groo] from the band structure of half – Heusler (see below for a description) NiMnSb. According to De Groot half – metals are materials having the Fermi level situated in the gap, for one spin direction. As a result, these materials would be 100% polarized at  $T = 0$  K. Moreover, due to total polarization at zero K, the electrical resistivity would be infinity for one spin direction in half – metallic materials making these materials promising candidates for spintronic devices: non – volatile magnetic random access memories, magnetic sensors [Pri], etc..

The full – Heusler alloy  $Mn_2VAI$  was the first one proposed to be a HMF and has been studied in detail both experimentally and theoretically [Ishi4,Itoh]. Although the Heusler alloys like NiMnSb, known as half or semi – Heusler compounds, have monopolized initially the interest of the experimentalists, in the last approximately five years the interest has been shifted to the so called full – Heusler compounds and mainly to the ones containing Co, like  $Co_2MnAl$ . These alloys are known from 1971, when Webster [Web] managed to synthesize Heusler alloys containing cobalt.

In this work, the results of our studies, both experimental and theoretical, of the effects of the rare – earths substitutions on the physical properties of different half or full – Heusler alloys will be presented.

### A.1 Structural properties of Heusler alloys

As mentioned above, two distinct families of Heusler compounds are known, one with 1:1:1 (half – Heusler) and the other one with 2:1:1 (Heusler) stoichiometry. The generic formula for the first compound is  $XYZ$  and half – Heusler alloys usually crystallize in a non – centrosymmetric cubic structure, space group no. 216,  $F\bar{4}3m$ , ( $C1_b$ ) which can be derived from the tetrahedral ZnS – type structure by filling the octahedral lattice sites. The corresponding Wyckoff positions are  $4a$  (0, 0, 0),  $4b$  (1/2, 1/2, 1/2), and  $4c$  (1/4, 1/4, 1/4). The Heusler compounds  $X_2YZ$  crystallize in the cubic space group  $Fm\bar{3}m$  (space group no. 225) with  $Cu_2MnAl$  ( $L2_1$ ) as prototype [Heus2, Heus3]. The  $X$  atoms occupy the Wyckoff position  $8c$  (1/4, 1/4, 1/4) while the  $Y$  and the  $Z$  atoms are located at  $4a$  (0, 0, 0) and  $4b$  (1/2, 1/2, 1/2), respectively.

The lattice of all Heusler and half – Heusler alloys, shown in Fig.A.1.3, can be generally regarded as the combination of four interpenetrating f.c.c lattices.

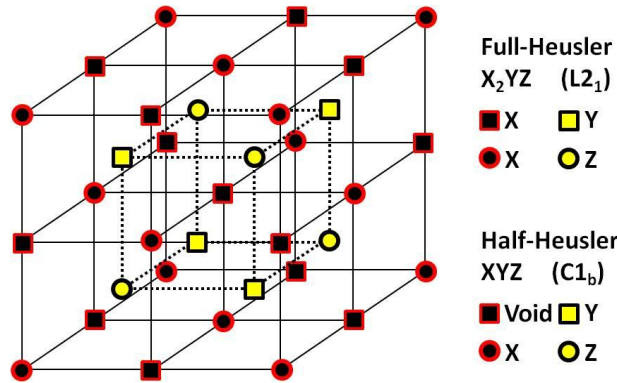


Fig. A.1.3 C1b and L21 type structures adopted by the half – and full – Heusler alloys.

When one of the X position is vacant the structure will be the C1<sub>b</sub> corresponding to the half – Heusler alloy.

**X<sub>2</sub>YZ Heusler compounds**

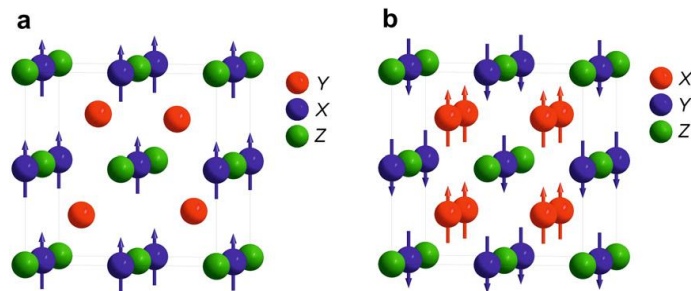
H 2.20																	He				
Li 0.98	Be 1.57															B 2.04	C 2.55	N 3.04	O 3.44	F 3.98	Ne
Na 0.93	Mg 1.31															Al 1.61	Si 1.90	P 2.19	S 2.58	Cl 3.16	Ar
K 0.82	Ca 1.00	Sc 1.36	Ti 1.54	V 1.63	Cr 1.66	Mn 1.55	Fe 1.83	Co 1.88	Ni 1.91	Cu 1.90	Zn 1.65	Ga 1.81	Ge 2.01	As 2.18	Se 2.55	Br 2.96	Kr 3.00				
Rb 0.82	Sr 0.95	Y 1.22	Zr 1.33	Nb 1.60	Mo 2.16	Tc 1.90	Ru 2.20	Rh 2.28	Pd 2.20	Ag 1.93	Cd 1.69	In 1.78	Sn 1.96	Sb 2.05	Te 2.10	I 2.66	Xe 2.60				
Cs 0.79	Ba 0.89	Hf 1.30		Ta 1.50	W 1.70	Re 1.90	Os 2.20	Ir 2.20	Pt 2.20	Au 2.40	Hg 1.90	Tl 1.80	Pb 1.80	Bi 1.90	Po 2.00	At 2.20	Rn				
Fr 0.70	Ra 0.90																				
		La 1.10	Ce 1.12	Pr 1.13	Nd 1.14	Pm 1.13	Sm 1.17	Eu 1.20	Gd 1.20	Tb 1.10	Dy 1.22	Ho 1.23	Er 1.24	Tm 1.25	Yb 1.10	Lu 1.27					
		Ac 1.10	Th 1.30	Pa 1.50	U 1.70	Np 1.30	Pu 1.28	Am 1.13	Cm 1.28	Bk 1.30	Cf 1.30	Es 1.30	Fm 1.30	Md 1.30	No 1.30	Lr 1.30					

Fig. A.1.4. Elements which form the half – and full – Heusler alloys [Graf].

The elements which form these Heusler alloys are presented in Fig. A.1.4. One can observe that these Heusler alloys are a combination of transition and poor metals (or non – metals) but heavy rare – earths can also form these structures, making them interesting from magnetic point of view.

## A.2 Magnetic properties of Heusler alloys

The XYZ materials have only one magnetic sublattice since only the atoms on the octahedral sites can carry a magnetic moment, as indicated in Fig. A2.1. Magnetic XYZ Half – Heusler materials exist only for  $X = \text{Mn}, \text{Co}$  and RE. This results from the localized nature of the four 3d electrons of  $\text{Mn}^{3+}$  and of the 4f electrons, respectively, which carry the magnetic moment. However, experimentally, a small induced magnetic moment is also found on Nickel and the late transition metals. Among the RE containing Heusler compounds known in the literature, most of the compounds are semiconductors or semimetallic systems, antiferromagnets with low Néel temperatures [Gofr, Casp]. Since the magnetic ions occupy the NaCl – sublattice, their distance between them is quite large, which hints at a magnetic interaction based on a super – exchange mechanism. Only very few ferromagnetic Half – Heusler compounds containing RE are described in literature, like NdNiSb.[Heyn, Hart]. The Mn containing Half – Heusler compounds are half – metallic ferromagnets with high Curie temperatures.



**Fig. A.2.1.** (a) XYZ Half – Heusler compounds exhibit only one magnetic sublattice since only the atoms on the octahedral sites carry a localized magnetic moment. (b)  $X_2YZ$  Heusler compounds, however, have two magnetic sublattices which can couple ferro- or antiferromagnetically.[Graf]

In the  $X_2YZ$  Heusler compounds the situation is completely different because of the two X atoms occupying the tetrahedral sites which allows a magnetic interaction between the X atoms and the formation of a second – more delocalized – magnetic sublattice (compare Fig.A2.1). Due to the two different magnetic sublattices, the  $X_2YZ$  Heusler compounds can show all kind of magnetic ground states: ferromagnetic, ferrimagnetic, and half – metallic ferromagnetism. The majority of Heusler alloys are ferromagnets that saturate in an applied magnetic fields of less than 5 kOe at low temperatures, but there are also antiferromagnets too, mostly among the alloys containing Mn at the Y sites.

## **B. Experimental techniques for the preparation and characterization of half – metals.**

### **B.1 Preparation of bulk samples by arc melting technique and by levitation.**

#### **B.1.1 Arc melting**

The half – metals investigated in the present work were prepared by the arc melting of appropriate amounts of constituent high purity elements using the electrical arc melting furnace of the Institute of Physics of the Babes – Bolyai University. For a better homogeneity of the samples several melting procedures were performed on both sides of the half – metal. High purity, more than 99.9 % purity elements were used as beginning constituents. We took into account also the high oxidation level of the rare earth elements by cleaning them only just before they were introduced in the furnace. In some cases, in order to eliminate the stresses and to obtain homogeneous single – phase samples the ingots were thermally treated.

#### **B.1.2 Induction and levitation furnace**

Induction heating is a method for heating electrically conductive materials. In 1831 Michael Faraday invented the solenoid and independently discovered the principle of induction, leading to the understanding and exploitation of the related heating effects. The temperature is dependent on the material intrinsic properties like resistivity, permeability, specific heat and the magnetic field. Some of the studied samples were prepared by induction and levitation furnace.

## **B.2 Structural characterization of half metals.**

### **B.2.1 Structural characterization of half – metals by X – Ray diffraction.**

For the structural characterization of our samples we have used the Bruker D8 Advance X – Ray diffractometer existent at the Babes – Bolyai University, Institute of Physics. The measurements are computer assisted and quite automatized. The samples are investigated in the Brag – Brentano geometry. The result of the experiment is the X-Ray pattern of the investigated compound. Using appropriate software, one can then proceed to a qualitative/quantitative analysis of the experimental results: structure of the sample, phase determination, cell parameter refinement, Rietveld refinement, etc..

### **B.2.2 Structural characterization of half – metals by Transmission Electron Microscopy**

In order to gain more insight on the structural properties of our samples we have used the Transmission Electron Microscopy (TEM) and the Selected Area Electron Diffraction (SAED) techniques. If the used microscope is equipped with analytical analysis setup, like EDS (energy dispersive spectroscopy) or EELS (electron energy loss spectroscopy) the microscope is named as analytical one (AEM). This experimental setup was used to create a more complex database on the studied half-metallic systems.

### **B.3 Electrical characterization of half – metals by the four point probe method.**

In the case of semiconductors and metals, one of the quickest and relatively simple methods for measuring the electrical resistivity is the four point probe technique. It also offers valuable information about the transition temperature of the investigated sample. This four point probe technique was used to investigate the electrical properties of our half-metals.

#### **B.3.1 Determination of magnetoresistance of Heusler alloys.**

In our laboratory a Cryogenic Resistivity Measuring System is available. The RnX series measurement systems provide a versatile platform for a wide range of studies into the properties of materials as a function of temperature, time and magnetic field. This system includes DC and AC resistivity, magnetisation and susceptibility. The standard RnX series enable measurement of sample resistance in the range of  $10^6$  to  $10^{-6}$  Ohms in a temperature range of 1.6 to 300K. If measurements are required in a magnetic field the system is suitable for every need providing up to 7T. Resistance measurements are made using a 4 terminal probe with drive currents from 1A up to 100mA. The sensitivity of the data acquisition system is 0.1 V to 1000mV full scale. In order to verify each measurement, the system simultaneously measures both the 2 and 4 – terminal voltages over the sample. The applied voltage is dynamically reversed in order to subtract thermal potentials, and the measurement averaged [Cry].

### **B.4 Magnetic characterization of half – metals by vibrating sample magnetometer**

Magnetic measurements in fields up to 12T and temperature range of 4.2–900K were performed on all the samples at the Babes-Bolyai University. At low temperatures (below 300K) a vibrating magnetometer (VSM – Cryogenic) is used to measure the spontaneous

magnetization of the samples and to determine the Curie temperature and the value of the spontaneous magnetization at 0K by extrapolation. At high temperatures (above the Curie temperature) the variation of the magnetic susceptibility with the temperature was obtained using a Weiss balance in the 300 – 900K temperature range and magnetic fields up to 1T. The magnetic characterization of the investigated systems is realized by correlating the data from both ordered and paramagnetic states, which allowed the calculation of magnetic moments and the contribution of each element to the total magnetization of the compound.

### **B.6 Electronic structure of half – metals revealed by X – ray photoelectron spectroscopy**

The electronic structure of the materials is investigated by X – ray photoelectron spectroscopy. The XPS experiments were performed using a commercially available spectrometer PHI Model 5600 Multi-Technique System produced by the Perkin Elmer Corporation, located at the Osnabrück University. XPS measurements were used to determine: core levels, chemical shifts, valence band levels, multiplet splitting, shake – up and shake – off satellites of the studied half-metals.

### **B.7 Electronic structure calculations**

Two types of theoretical computations were used in order to calculate the band structure of the parent and RE doped half-metallic systems. In case of the  $X_2YZ$  type Heusler alloys the density functional theory (DFT), with the LSDA approximation, was used to compute the DOS and the magnetic moments on the atoms in ferromagnetic and antiferromagnetic coupling.

In case of half-Heusler compounds, the electronic structure of the alloys and compounds in the ferromagnetic state were calculated self – consistently by means of the spin polarized relativistic Korringa–Kohn–Rostocker (KKR) method in the atomic sphere approximation (ASA) mode [Wein,Goni,Stra]. Several different properties can be investigated by means of the SPRKKR package on the basis of the fully relativistic electronic structure calculation, especially response functions and spectroscopic properties.[Pacu]



## C. Physical properties of full – Heusler alloys

Chapter C contains the investigations physical properties of the full-Heusler and RE doped Heusler alloys. The studied system is the  $\text{Co}_2\text{M}_{1-x}\text{RE}_x\text{A}$  where M – are metals like Mn or Cr, RE – are the lanthanide impurities like Gd, Tb, Dy, Ho,Er and A – are the nonmetallic components like Si or Al. It is important to prove that after the lanthanides substitution the structure will remain the same.

### C.1 Structural properties of full – Heusler alloys

#### C.1.1 Sample preparation

$\text{Co}_2\text{MnSi}$  and  $\text{Co}_2\text{Mn}_{1-x}\text{RE}_x\text{Si}$  compounds with  $x=0, 0.01, 0.05,$  and  $0.1$  and RE=Gd, Ho, and Tb were prepared by arc melting high purity ingots of the constituent elements. The ingots were remelted several times in order to ensure a good homogeneity. The samples were heat treated in vacuum, at  $1000\text{ }^\circ\text{C}$ , for 5 days.

#### C.1.2 X – Ray diffraction structural analysis of full – Heusler alloys

The crystallographic structure of the prepared compounds was investigated by X – ray diffraction measurements on bulk powdered material. The FullProf program was used for Rietveld analysis of the X – ray diffraction data collected for all of the studied Heusler alloys.

The X – ray diffraction pattern of the undoped  $\text{Co}_2\text{MnSi}$  is presented in Fig. C.1.2.1.

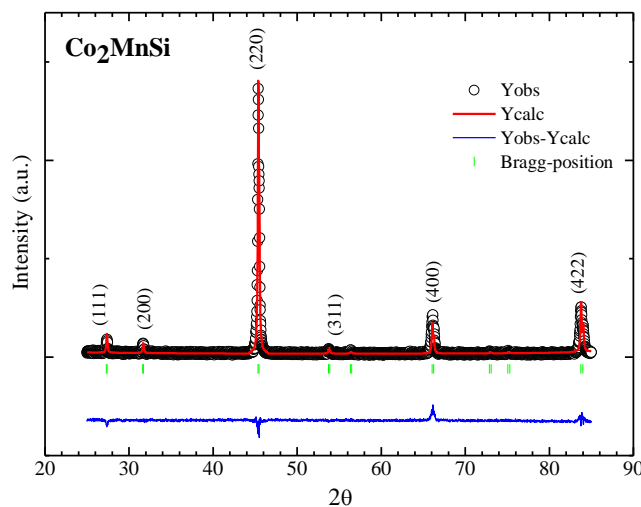


Fig. C.1.2.1 XRD pattern of undoped  $\text{Co}_2\text{MnSi}$

The Rietveld analysis shows, in the limit of experimental errors, that the investigated compound is single phase with  $\text{BiF}_3$  – type structure, crystallized in a cubic structure having  $Fm\bar{3}m$  space group. The cell parameter was found to be 5.654 Å.

The X-ray diffraction pattern of the Gd ( $x=0.01$ ) doped sample is presented in Fig. C1.2.2. It was proved by Rietveld analysis that  $\text{BiF}_3$ -type structure was formed. XRD – studies suggest us that the Gd entered into the transition metal sublattice of  $\text{Co}_2\text{MnSi}$ , similar results was found for ( $x=0.05$ ) of the Gd concentration.

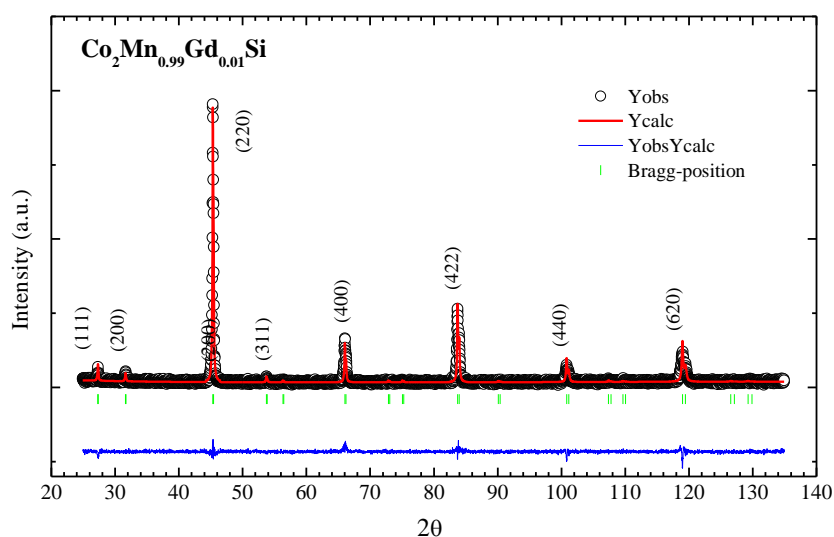


Fig. C.1.2.2 XRD pattern of  $\text{Co}_2\text{Mn}_{0.99}\text{Gd}_{0.01}\text{Si}$

Similar results were obtained for  $\text{Co}_2\text{Mn}_{1-x}\text{Tb}_x\text{Si}$  alloys, but only for small Tb doping ( $x=0.01$ ). The X – ray analysis shows, in the limit of experimental errors, that  $\text{Co}_2\text{Mn}_{0.99}\text{Tb}_{0.01}\text{Si}$  is single phase with  $\text{BiF}_3$  – type structure. The lattice parameter is  $a=0.5653\pm 0.001$  nm and is very little affected by substitution, probably due to the low Tb concentrations. The compounds with  $x=0.05$  and  $x=0.1$  were found to be not single phase.

### C.1.3 Transmission electron microscopy study of $\text{Co}_2\text{MnSi}$ and $\text{Co}_2\text{Mn}_{0.9}\text{Tb}_{0.1}\text{Si}$

For the registration of the image of parallel thin samples and for elaboration of electron diffraction patterns, transmission electron microscope was used. In Fig. C.1.3.1 TEM and SAED image of  $\text{Co}_2\text{MnSi}$  is presented.

During TEM analysis HREM images and elemental mappings of the studied samples were made. All the results confirm that the samples are homogeneous and the desired structures were formed.

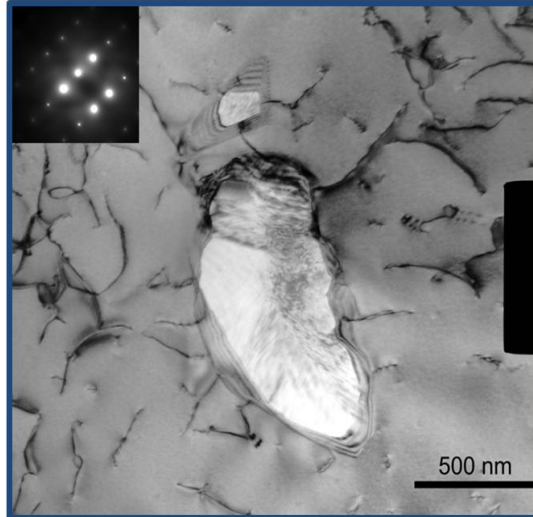


*Fig. C.1.3.1 TEM and SAED pattern of Co<sub>2</sub>MnSi*

Selected area electron diffraction pattern shown that the analyzed sample can be identified as Co<sub>2</sub>MnSi (30 – 0447 card of JCPDFWIN) BiF<sub>3</sub> type cubic structure. Small inclusions were revealed. Because are dispersed in the bulk, these small inclusions are not influencing the physical properties of the alloy.

The TEM image of Co<sub>2</sub>Mn<sub>0.9</sub>Tb<sub>0.1</sub>Si is presented in Fig.C.1.3.2. As it is seen is in case of substitution of Mn atoms with Tb needle structure are formed. EDS analysis revealed that the lamellar structure is rich in Tb.

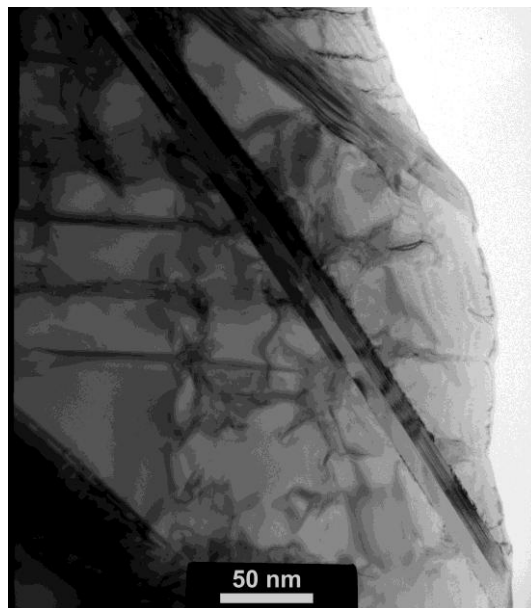


*Fig. C.1.3.2 TEM image of Co<sub>2</sub>Mn<sub>0.9</sub>Tb<sub>0.1</sub>Si*

## C.2 XPS investigations on full – Heusler alloys.

Fig. C.2.1 shows the XPS spectra of  $\text{Co}_2\text{Mn}_{0.99}\text{Gd}_{0.01}\text{Si}$  recorded for binding energies between 95 eV and 170 eV. In this spectral region the Si 2p, Co 3s, Gd 4d and Si 2s core levels can be analyzed. The spectrum was normalized to the Co 3s core level and the XPS spectra of pure Gd is shown for comparison. One can see that Gd 4d core level in  $\text{Co}_2\text{Mn}_{0.99}\text{Gd}_{0.05}\text{Si}$  is shifted to higher binding energy compared to the position in pure Gd which allows us to consider that Gd atoms occupy positions in the lattice and not interstitial.

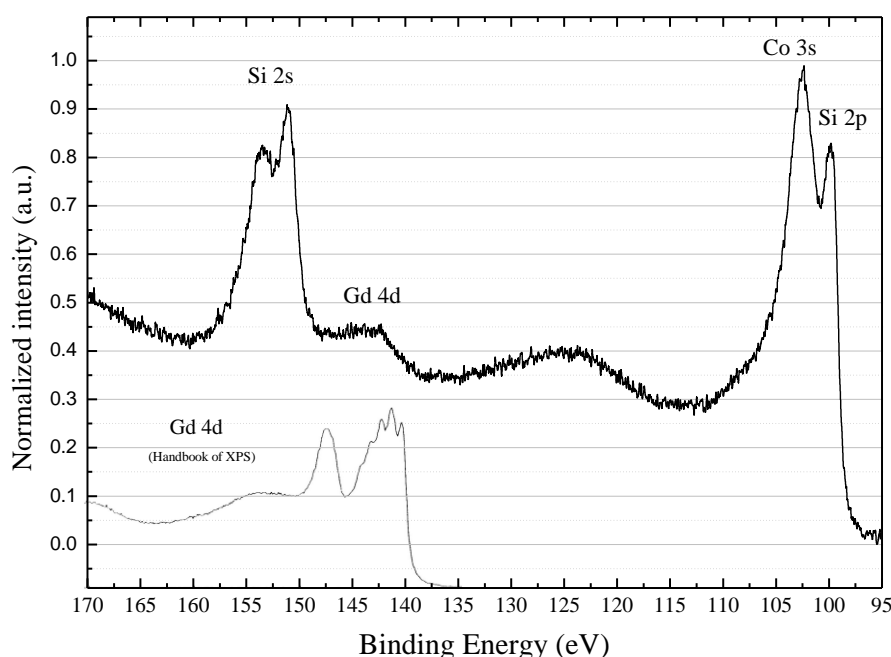


**Fig. C.2.1** XPS spectra of  $\text{Co}_2\text{Mn}_{0.9}\text{Gd}_{0.1}\text{Si}$

In table C.2.1 the theoretical intensities of the Gd 4d and Si 2s core levels, calculated relative to the Co 3s core level, are compared to the experimental values estimated from fig. C.2.1. The calculated and experimental values are close and indicate the good quality of the sample.

**Table C.2.1** The calculated concentrations of the rare earth elements in  $\text{Co}_2\text{Mn}_{0.99}\text{Gd}_{0.05}\text{Si}$

Core level	Binding Energy (eV)	Cross section	Concentration	Theoretical intensity	Experimental intensity
Co 3s	102.5	0.011	2	1	1
Gd 4d	142.5	0.142	0.01	0.065	0.09
Si 2s	151.2	0.013	1	0.59	0.48

### C.3 DOS calculations for full – Heusler alloys

Based on experimentally determined lattice constants, we have computed the band structures of  $\text{Co}_2\text{Mn}_{0.875}\text{Ho}_{0.125}\text{Si}$  and  $\text{Co}_2\text{MnSi}$  compounds using a supercell eight times greater than unit cell. A d–f – type model was used in the mean field approximation, in which the Mn 3d and Ho 4f states were described by LDA + U method, whereas the 3d–4f interaction was treated as perturbation.

The calculated DOS of  $\text{Co}_{16}\text{Mn}_8\text{Si}_8$  and  $\text{Co}_{16}\text{Mn}_7\text{HoSi}_8$  are presented in Fig. C.3.1.

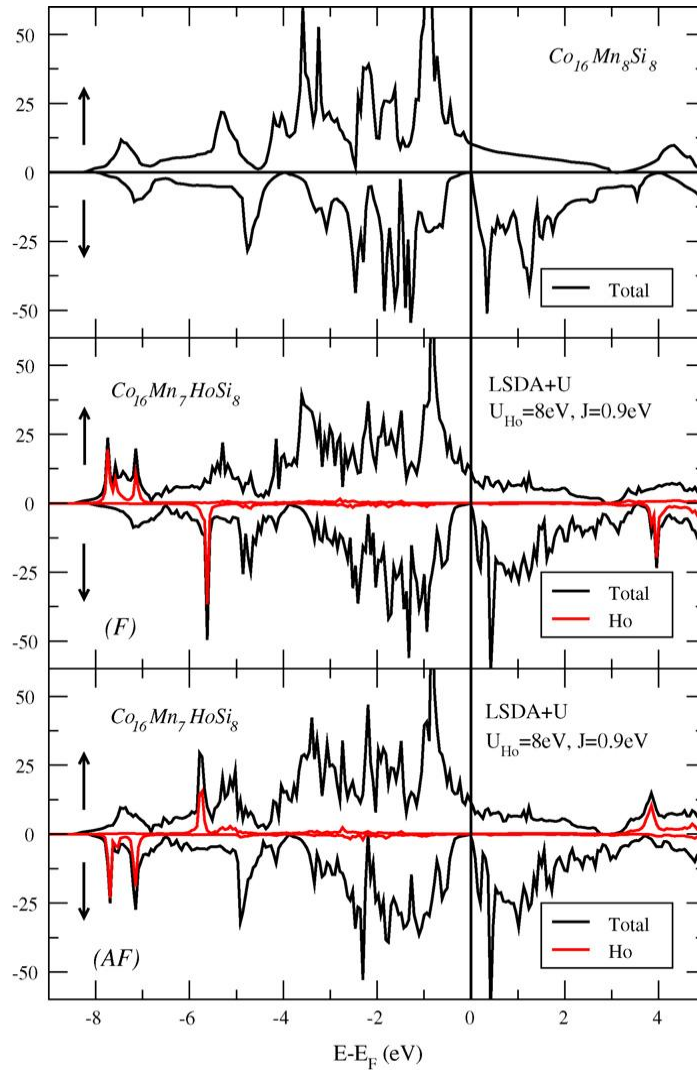


**Fig. C.3.1** DOS of  $\text{Co}_2\text{MnSi}$  and  $\text{Co}_{16}\text{Mn}_7\text{HoSi}_8$

The analysis of the band structures of the doped alloy shows that the half – metallic properties are completely conserved, if Ho substituted Mn sites. Table C.3.1 shows the atomic magnetic moments for the pure compound and data obtained for the Ho – doped sample. A diminution of Co moment is shown, as result of doping effect.

**Table C.3.1** The atomic magnetic moments (in  $\mu_B/\text{atom}$ ) for the pure compound and in the presence of Ho impurities

$\text{Co}_{16}\text{Mn}_8\text{Si}_8$	LSDA	
$M_{\text{Co1}}$	1.00	
$M_{\text{Co2}}$	1.00	
$M_{\text{Mn}}$	3.03	
$M_{\text{Si}}$	0.03	
$\text{Co}_{16}\text{Mn}_7\text{HoSi}_8$	LSDA+U	
	AF	F
$M_{\text{Co1}}$	0.9636	0.9652
$M_{\text{Co2}}$	0.9636	0.9652
$M_{\text{Mn}}$	2.9848	2.9821
$M_{\text{Ho}}$	-4.1189	3.8827
$M_{\text{Si}}$	-0.0241	-0.0250

In order to check the influence of heavy rare earths on the electronic and magnetic properties of the full heusler alloys we have considered the Gd substitution. Similar results were obtained for Gd substitution too.

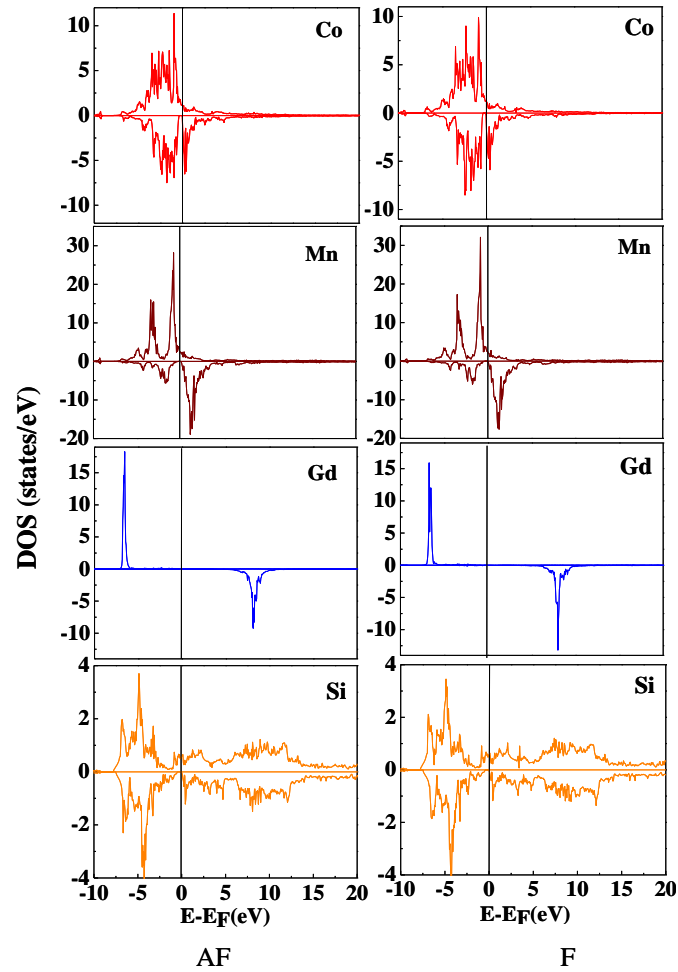


**Fig. C.3.4** Partially DOS for  $\text{Co}_{16}\text{Mn}_7\text{GdSi}_8$  in case of antiferromagnetic and ferromagnetic coupling

The strength of such a coupling was evaluated by calculating, in an *ab initio* fashion, the total energy of  $\text{Co}_{16}\text{Mn}_7\text{GdSi}_8$  compound for a parallel and antiparallel *f-d* coupling. The *f-d* coupling constant was calculated as the  $E_{\text{Ferro}} - E_{\text{Antiferro}}$  energy corresponding to a Gd (4*f*)–Mn (3*d*) pair and has values of 54 K for  $U = 7$  eV,  $J = 0.7$  eV and 105 K for  $U = 3$  eV,  $J = 0.7$  eV. One can see that the minimum energy is in the case of an antiparallel coupling between Mn (3*d*) and Gd (4*f*) spins as it is expected for heavy rare – earths–3*d* transition metals compounds [Bur]. Similar results was found for the case of Tb doped samples. DOS calculations were in good agreement with the experimental results for the case on AF coupling.

#### C.4 Magnetic investigations on full – Heusler alloys (VSM measurements)

Magnetic measurements on  $\text{Co}_2\text{Mn}_{0.9}\text{Ho}_{0.1}\text{Si}$  and  $\text{Co}_2\text{MnSi}$  compounds were performed in the temperature range 4.2–990 K and external fields up to 12 T. The spontaneous magnetizations,  $M_s$ , were determined from magnetization isotherms according to approach to saturation law (Ec. B4). The magnetization isotherms for  $\text{Co}_2\text{Mn}_{1-x}\text{Ho}_x\text{Si}$  recorded at 4.2 K are shown in Fig.C.4.1.

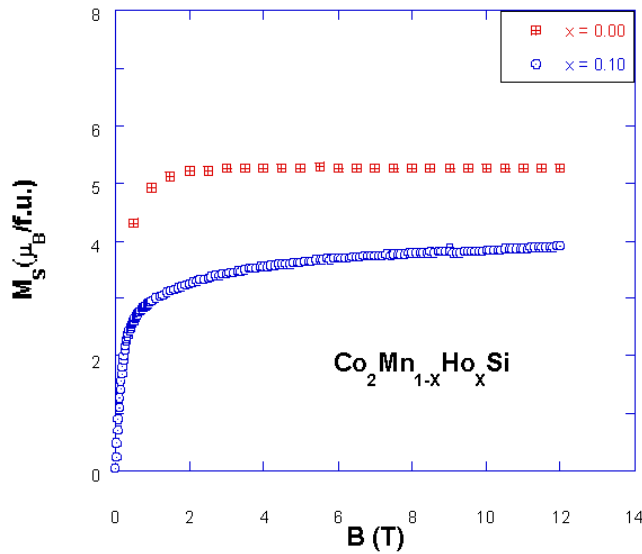


Fig. C.4.1 Magnetization isotherms at 4.2 K

One can see that the parent sample is saturated in external field of 3 T while in the case of sample with Ho the saturation is not reached even in 9 T field. Therefore, the experimental moments were obtained according to approach to saturation law. The values obtained for  $\text{Co}_2\text{MnSi}$  and  $\text{Co}_2\text{Mn}_{0.9}\text{Ho}_{0.1}\text{Si}$  are  $5.07\mu_B/\text{f.u.}$  and  $3.52\mu_B/\text{f.u.}$  respectively.

These results are in very good agreement with the DOS calculated values obtained for an antiferromagnetic coupling of the Mn and Ho magnetic moments. The above data suggest that some Ho can enter in  $\text{Co}_2\text{MnSi}$  lattice. Similar results were obtained for all doped samples.

### C.5 Electrical properties of full – Heusler alloys

Examining the very low – temperature resistivity data half – metallic properties of Heusler alloys can be probed. The electrical measurements by four probe method were made at the Babes – Bolyai University. The temperature dependence of electrical resistivity of  $\text{Co}_2\text{Mn}_{1-x}\text{Tb}_x\text{Si}$  ( $x=0.05$ ) is presented in Fig. C.5.1.

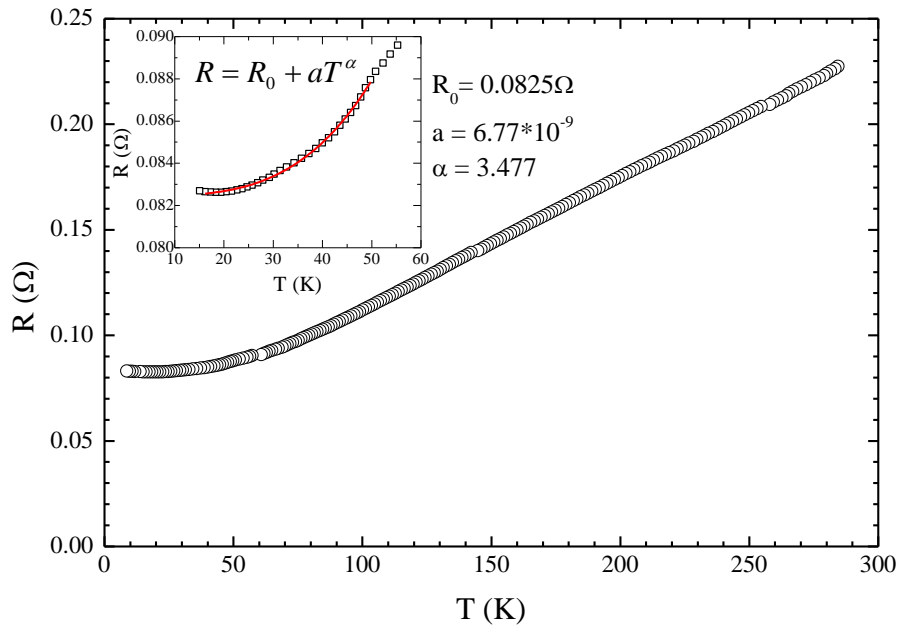


**Fig. C.5.1** The temperature dependence of electrical resistivity of  $\text{Co}_2\text{Mn}_{1-x}\text{Tb}_x\text{Si}$ ; the inset contains the fitting of the low temperature data ( $T < 50$  K).

In our case the temperature variation of electrical resistance data in the low temperature region was fitted with the expression:

$$R = R_0 + aT^\alpha \quad (\text{C8})$$

If  $\alpha$  is 2 the presence of spin – flip scattering is probed and the material is not half metal ferromagnet. In our case  $\alpha \approx 3.5$ .



## C.6 Conclusions on the physical properties of full – Heusler alloys

- The  $\text{Co}_2\text{MnSi}$  and all RE substituted  $\text{Co}_2\text{Mn}_{1-x}\text{RE}_x\text{Si}$  (with x between 0 and 0.1 and RE = Ho, Gd, Tb) compounds were prepared by arc melting the constituent elements in a purified argon atmosphere.
- XRD structural investigation revealed that, in the limit of experimental errors, the investigated compounds are single phase with  $\text{BiF}_3$  – type structure, crystallized in a cubic structure having  $Fm\bar{3}m$  space group. In case of Tb substitution it was found that if the dopant concentration increases ( $x > 0.01$ ) a second crystallographic phase is present in the sample.
- TEM analysis of the studied full – Heusler alloys revealed that the formed alloys are homogeneous; only few inclusions were found. Because they are dispersed in the bulk, these small inclusions are not influencing the physical properties of the alloy. For  $\text{Co}_2\text{Mn}_{0.95}\text{Tb}_{0.05}\text{Si}$  a secondary lamellar, Tb rich phase was identified from TEM analysis complemented with EDS.
- From the HREM images the lattice parameter  $5.653 \text{ \AA}$  can be determined for the parent compound  $\text{Co}_2\text{MnSi}$ . In the elemental mapping of this alloy, a good homogeneity of the sample is observable and no isolated islands can be revealed.
- XPS analysis revealed the good quality of the sample. The position of the Gd 4d core level in  $\text{Co}_2\text{Mn}_{0.99}\text{Gd}_{0.05}\text{Si}$  (shifted to higher binding energy compared to the position in pure Gd) indicates that Gd atoms occupy positions in the lattice.
- DOS calculations of the band structures of the doped alloy shows that the half – metallic properties are not affected if RE atoms substitute the manganese ones. This effect is not determined by the spin–orbit interaction, but through the coupling between the RE (4f) spin with the Mn (3d) itinerant electron spins. The electronic structure calculations suggest that the half – metallicity is preserved when RE atoms substitutions occupy Mn sites.
- The  $f$ – $d$  coupling constant was calculated for all investigated alloys as the  $E_{\text{Ferro}} - E_{\text{Antiferro}}$  energy corresponding to a RE (4f) – Mn (3d) pair for  $U=9 \text{ eV}$ ,  $J=0.9 \text{ eV}$

and for  $U=7$  eV,  $J=0.9$  eV. The minimum energy was found in the case of an antiparallel coupling between Mn ( $3d$ ) and RE ( $4f$ ) spins as expected for heavy rare – earths – 3d transition metals compounds.

- The magnetic moments obtained from magnetization measurements are in very good agreement with the calculated values obtained for an antiparallel orientation of rare earth and transition metals moments ( $U=7$  eV).
- The lack of  $T^2$  behavior of the temperature dependence of the electrical resistance data below 50 K, clearly indicates the absence of spin – flip scattering. In conclusion the half – metallic character of the material was proofed by electrical measurements too.

## D. Physical properties of half – Heusler alloys

In Chapter D the physical properties of the half-Heusler alloys are presented. NiMnSb crystallizes in the cubic structure of  $C1b$  type with space group  $F\bar{4}3m$ . This structure can be described as three interpenetrating fcc lattices of Ni, Mn, and Sb.

### D.1 Structural analysis of half – Heusler alloys

#### D.1.1 Sample preparation

The NiMn<sub>1-x</sub>RE<sub>x</sub>Sb compounds with  $x = 0, 0.05$  and RE = Gd, Dy, Ho, Er were prepared by arc melting the constituent elements in a purified argon atmosphere from high purity ingots. The ingots were remelted several times in order to ensure a good homogeneity. The samples were heat treated in vacuum at 1000 °C for 5 days.

#### D.1.2 X – Ray diffraction

The crystal structure was checked by X – ray Diffraction using a Bruker 8 XD diffractometer. The diffraction patterns for NiMnSb is presented in Fig.D1.2.1

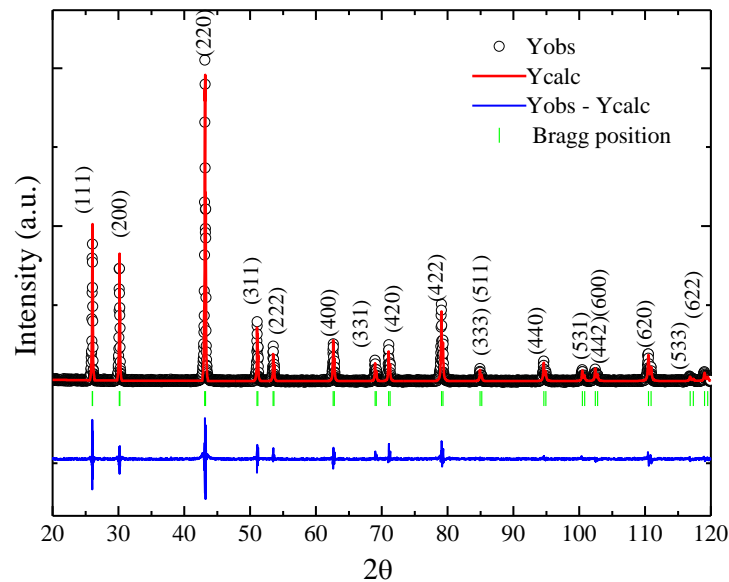
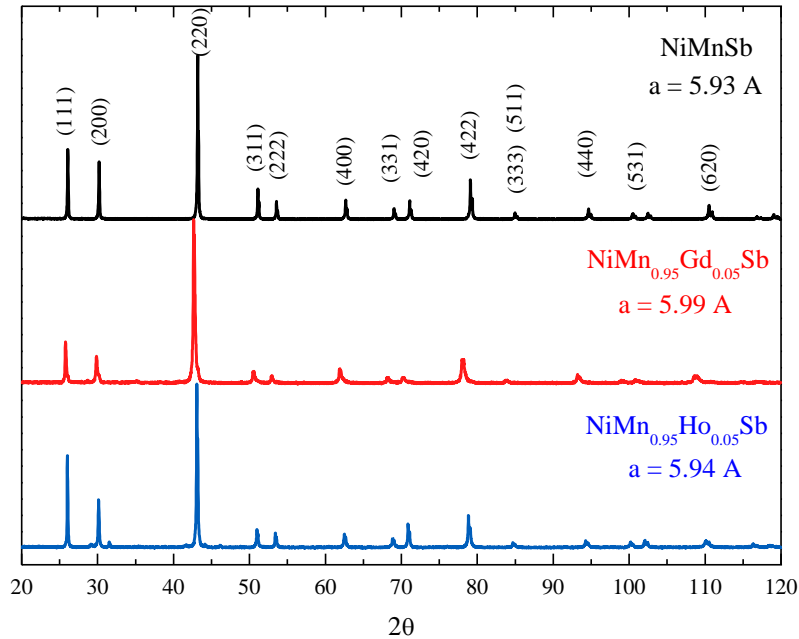


Fig. D.1.2.1 Diffraction pattern for NiMnSb

The X – ray analysis of NiMn<sub>1-x</sub>RE<sub>x</sub>Sb samples shows, in the limit of experimental errors, that the compounds are single phase with a  $C1b$  type cubic structure (space group  $F\bar{4}3m$ ). The lattice parameters increase from  $a=0.593$  nm ( $x=0$ ) to 0.594 nm

( $x=0.05$ ). This small increase could be explained by the higher ionic radius of RE atoms compared to Mn ion.

In Fig. D.1.2.3 a comparative representation of the diffraction patterns of NiMnSb, NiMn<sub>0.95</sub>Ho<sub>0.05</sub>Sb and NiMn<sub>0.95</sub>Gd<sub>0.05</sub>Sb is presented.



**Fig. D.1.2.3** XRD patterns of NiMnSb, NiMn<sub>0.95</sub>Ho<sub>0.05</sub>Sb and NiMn<sub>0.95</sub>Gd<sub>0.05</sub>Sb

All these XRD studies revealed that in case of NiMnSb half – Heusler compound an amount of  $x=0.05$  of Ho, Gd or Dy impurities can enter in the lattice. In the thesis the occupancy of the atomic positions are presented as a result of the Rietveld refinements. All the results of the refinements on the studied samples were in good agreement with other structural characterization methods, like XPS or TEM presented in upcoming chapters.

### D.1.3 TEM investigations of half – Heusler compounds.

The good homogeneity of the samples were revealed in TEM images of NiMn<sub>0.95</sub>Gd<sub>0.05</sub>Sb samples. In Fig.D.1.3.1 the BF – TEM image of NiMn<sub>0.95</sub>Gd<sub>0.05</sub>Sb is shown. As in case of Co<sub>2</sub>MnSi sample, presented in earlier chapter, TEM images of NiMn<sub>0.95</sub>Gd<sub>0.05</sub>Sb revealed the presence of small inclusions. Comparing our results with other characterization techniques, we conclude that the presences of this kind of small inclusions are not affecting the physical properties of the studied bulk half – Heusler alloys.

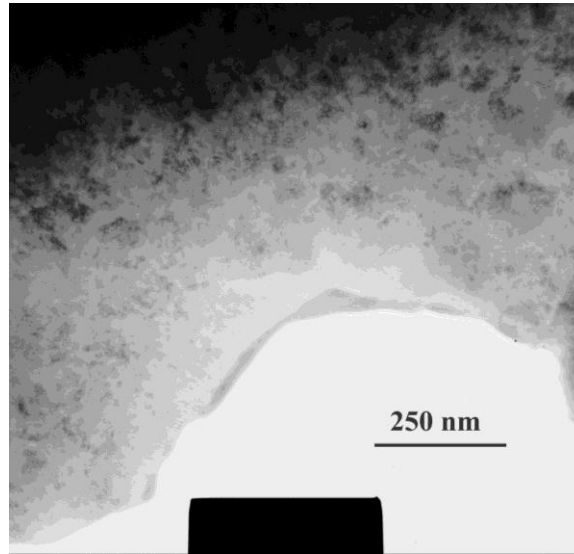


**Fig. D.1.3.1** TEM image of  $\text{NiMn}_{0.95}\text{Gd}_{0.05}\text{Sb}$

The EDS analysis of the sample revealed that the composition of these materials is corresponding to the expectations, and no other elements were detected.

## D.2 XPS investigations of half – Heusler compounds.

To illustrate the quality of the samples, the survey spectra were taken for all studied samples, with the identification of core – levels and Auger lines. The results suggest that contamination is almost absent, thus the XPS spectra is representative of the bulk. The survey spectra of pure  $\text{NiMnSb}$  is presented in Fig, D.2.1.

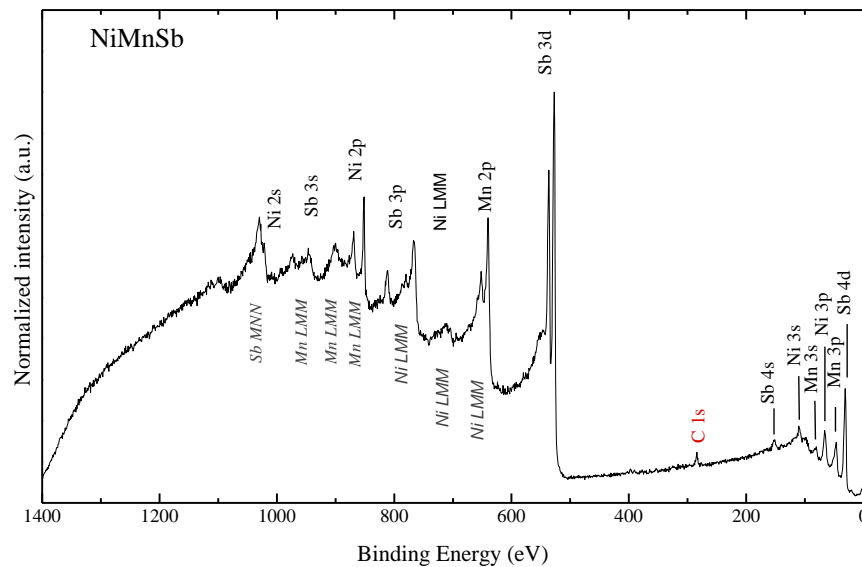


**Fig. D.2.1** Survey spectra of pure  $\text{NiMnSb}$ .

### D.2.1 XPS core level spectra

XPS core level and valence band spectra can provide important information on the electronic structure of 3d transition metal alloys and compounds.

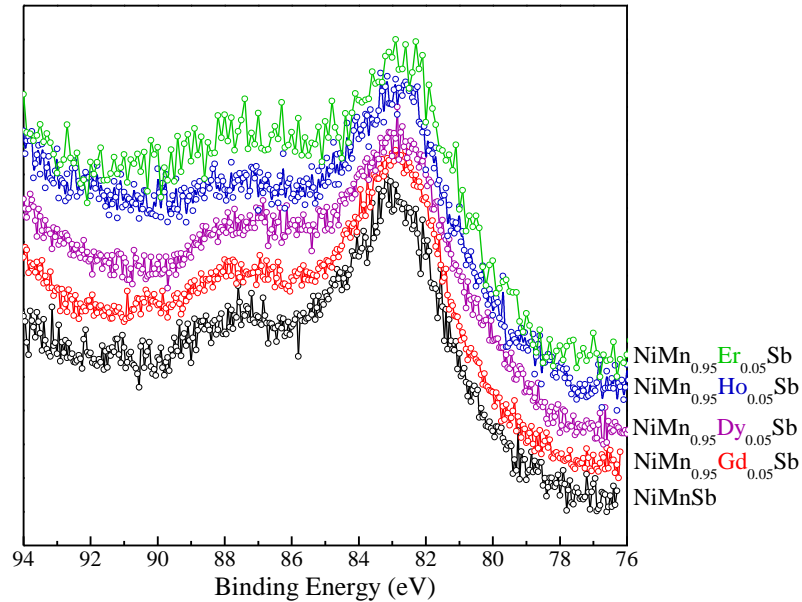


**Fig. D.2.1.1** (a) XPS Mn 3s core level spectra of  $\text{NiMn}_{0.95}\text{Ho}_{0.05}\text{Sb}$  obtained after the subtraction of a Shirley – type background [Shi]; (b) Ni 2p XPS spectra of  $\text{NiMn}_{0.95}\text{Ho}_{0.05}\text{Sb}$  and metallic Ni.

The multiplet splitting of the XPS core levels is a clear evidence of the existence of localized magnetic moments of transition metals. Therefore the splitting of the Mn 3s core level in all alloys was measured.

From the intensity ratio of the Sb 4s and the RE 4f peaks, the concentration of the rare earths in the  $\text{NiMn}_{0.95}\text{R}_{0.05}\text{Sb}$  alloys can be calculated. These calculated values of the concentrations, in each case of substituted sample are presented in Tab. D.2.1.2.

**Table D.2.1.2** The calculated concentrations of the rare earth elements in  $\text{NiMn}_{0.95}\text{R}_{0.05}\text{Sb}$

Core level	Cross section	Concentration	Theoretical int.	Exp. Int.
Sb 4s	0.011	1	1	1
Gd 4d	0.14	0.05	0.64	0.73
Ho 4d	0.14	0.05	0.75	0.5
Er 4d	0.14	0.05	1.03	0.57
Dy 4d	0.14	0.05	0.71	0.6

As it is seen in Table D.2.1.2, excepting the substitution of Er, in all substitution experiments the experimentally measured intensities are in a quiet good agreement with the theoretical ones, which means, that in the limit of the experimental errors, the substituting rare earth elements entered in the composition of the  $\text{NiMn}_{0.95}\text{RE}_{0.05}\text{Sb}$  alloy. We can conclude that XPS results on half – Heusler alloys are in good agreement with the XRD data. The substituting rare earth atoms entered in the alloy and they occupy a lattice position.

### D.2.2 XPS valence band spectra

In Fig.D.2.2.1 the comparative spectra of the valence band region of  $\text{NiMn}_{0.95}\text{RE}_{0.05}\text{Sb}$  with  $\text{RE} = \text{Ho}, \text{Gd}, \text{Dy}$  and  $\text{Er}$  dopants is presented. The Ni 3d cross section for Al  $K_{\alpha}$  radiation is about four times larger than the Mn 3d cross section, i.e. the valence – bands are dominated by the Ni 3d states. All alloys and compounds exhibit the Ni satellite separated by approximately 6 eV from the centroids of the valence bands, attributed to the presence of the d character in the unoccupied bands.

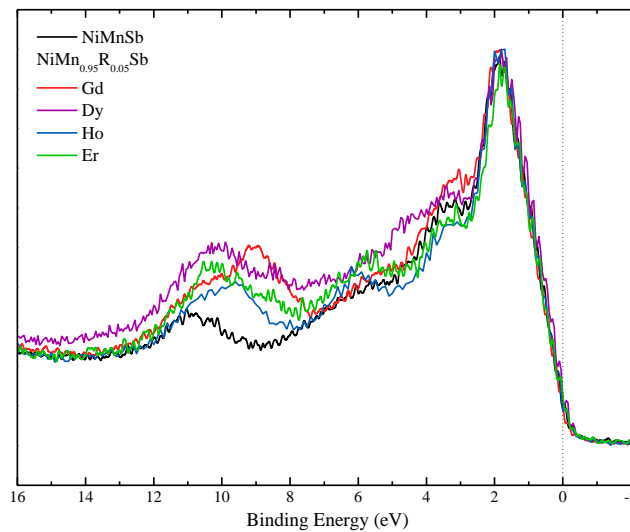


**Fig. D.2.2.1** XPS valence band spectra of  $\text{NiMnSb}$  and  $\text{NiMn}_{0.95}\text{RE}_{0.05}\text{Sb}$  alloys

The main difference between the valence band spectra of  $\text{NiMn}_{0.95}\text{RE}_{0.05}\text{Sb}$  and  $\text{NiMnSb}$  is between 8.5 eV and 10.5 eV, where the RE 4f states have a contribution. By subtracting the normalized XPS valence band spectra of  $\text{NiMnSb}$  from the normalized spectra of  $\text{NiMn}_{0.95}\text{RE}_{0.05}\text{Sb}$ , it was found that the binding energy of the RE 4f core level is  $\sim 9.5$  eV, at higher binding energy than in metallic rare earth. This indicates that the RE atoms occupy atomic positions in the  $\text{NiMnSb}$  cell.

For a good interpretation of the main characteristics of the valence band, the experimental spectra of NiMnSb and NiMn<sub>0.95</sub>R<sub>0.05</sub>Sb were compared with the calculated XPS valence band spectrum. In fig. D.2.2.3 the valence band region of the XPS spectra is presented in case of NiMnSb and NiMn<sub>0.95</sub>Ho<sub>0.05</sub>Sb. A good agreement between the computed and experimental results was observed. This indicates that the measured spectra are representative of the bulk.

All the experimental results in the valence band region suggest that in all substitution cases the rare earth atoms entered in the lattice and they are not forming second phases in the NiMn<sub>0.95</sub>RE<sub>0.05</sub>Sb alloys.

### D.3 DOS calculations on half – Heusler alloys

The calculated densities of states, (DOS), for Ni<sub>8</sub>Mn<sub>7</sub>GdSb<sub>8</sub> are presented in Fig.D.3.1.

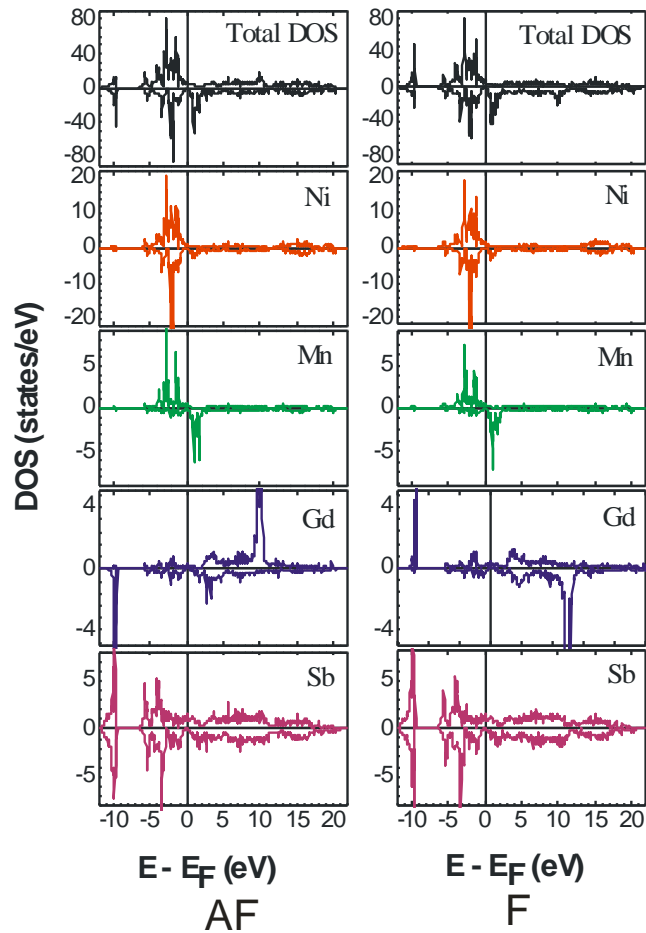


**Fig. D.3.1** Densities of states for Ni<sub>8</sub>Mn<sub>7</sub>GdSb<sub>8</sub> in case of antiferromagnetic respectively ferromagnetic coupling.



It was considered a ferromagnetic (F) respectively antiferromagnetic, (AF), coupling of Gd (*4f*) and Mn (*3d*) spins. The analysis of the band structures of the doped alloy shows that the half – metallic properties are completely conserved if gadolinium atoms substitute the manganese ones. This effect is determined by the coupling between the Gd (*4f*) spin and the Mn (*3d*) itinerant electron spins. Similar results were obtained in all RE substituted samples.

The average calculated atomic magnetic moments for the pure compound and data obtained for the Gd – doped sample are presented in Table D.3.1.

**Table D.3.1** The average calculated magnetic moments for  $\text{Ni}_8\text{Mn}_{8-x}\text{Gd}_x\text{Sb}_8$ .

<b>X; coupling</b>	<b>0</b>	<b>1; AF</b>	<b>1; F</b>
<b>M (Ni)</b> <b>(<math>\mu_B/\text{atom}</math>)</b>	– 0.28	– 0.234	– 0.206
<b>M (Mn)</b> <b>(<math>\mu_B/\text{atom}</math>)</b>	– 3.748	– 3.798	– 3.784
<b>M (Ho)</b> <b>(<math>\mu_B/\text{atom}</math>)</b>	–	7.214	– 7.061
<b>M (Sb)</b> <b>(<math>\mu_B/\text{atom}</math>)</b>	0.068	0.060	0.059
<b>M (void)</b> <b>(<math>\mu_B/\text{atom}</math>)</b>	– 0.04	– 0.029	– 0.043

A small modification of the magnetic moments was found as a result of doping. The calculated magnetic moments are  $4.00 \mu_B/\text{f.u.}$  (NiMnSb) and  $2.62 \mu_B/\text{f.u.}$  (AF coupling), respectively  $4.38 \mu_B/\text{f.u.}$  (F coupling) for  $\text{Ni}_8\text{Mn}_7\text{GdSi}_8$  compound.

#### **D.4 Magnetic properties of half – Heusler alloys.**

For the beginning, the relation between the magnetization as a function of the temperature, of pure NiMnSb and the dopant RE element, for Gd, Dy, Ho and Er concentration of  $x=0.05$ , was studied. The measurements were performed using a Weiss – Forrer method based equipment. All magnetic measurements were performed in the Babes – Bolyai University, Faculty of Physics Laboratory. The temperature dependences of the magnetizations in approx. 0.2 T applied magnetic field are shown in Fig. D.4.1.

The Curie temperatures were determined from the minimum of  $dM/dT$  dependences, presented in Fig.D.4.2.

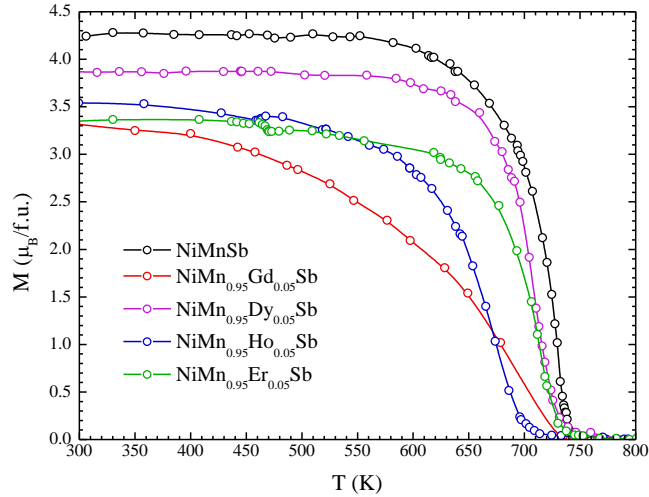


**Fig. D.4.1** The temperature dependence of the magnetization of NiMnSb and NiMn<sub>0.95</sub>RE<sub>0.05</sub>Sb alloys measured in 0.2T external magnetic field

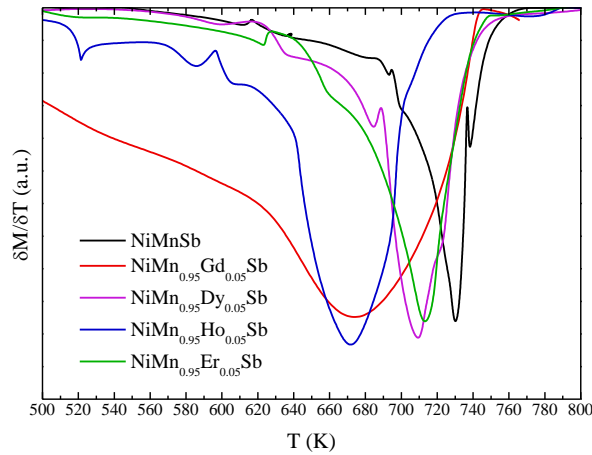


**Fig. D.4.2** The temperature dependences of  $dM/dT$  for NiMnSb and NiMn<sub>0.95</sub>RE<sub>0.05</sub>Sb samples.

Three types of interactions have to be considered: Mn – Mn, RE – Mn and RE – RE. Usually, the RE-RE interaction in 3d transition metals RE – M intermetallic compounds are negligible [Bur] while the RE – M interactions are weak comparing with M – M ones. In these compounds, the Curie temperature is determined mainly by the M – M. The partially substitution of M atoms with RE ones will weaken the M – M interactions and consequently the transition temperature will decrease. The Curie temperature of the NiMnSb was determined to be  $T_C = 729,3$  K which is in a very good agreement with value from the literature,  $T_{C(\text{theor})} = 730$  K [Borc]. The experimental results from Table D.4.1.shows that  $T_C$  of NiMn<sub>1-x</sub>RE<sub>x</sub>Sb decreases until 673 K, as a consequence of partially substitution of the M atoms.

**Table D.4.1** Curie temperature in NiMnSb and all substituted compounds

Compound	$T_C$
NiMnSb	729.29
NiMn <sub>0.95</sub> Er <sub>0.05</sub> Sb	711
NiMn <sub>0.95</sub> Dy <sub>0.05</sub> Sb	710
NiMn <sub>0.95</sub> Gd <sub>0.05</sub> Sb	678
NiMn <sub>0.95</sub> Ho <sub>0.05</sub> Sb	673

The magnetization isotherms, at 4.2 K, are shown in Fig. D.4.3. From the magnetization isotherms at 4.2 K the spontaneous magnetization values were determined. The obtained experimental values are  $4.07 \mu_B/\text{f.u.}$  ( $x=0$ ) respectively  $3.59 \mu_B/\text{f.u.}$  ( $x=0.05$ ).

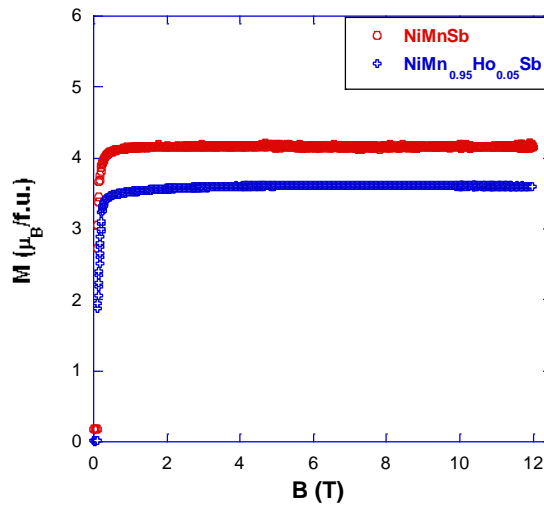


**Fig. D.4.3** Magnetization isotherms at 4.2 K of NiMnSb and NiMn<sub>0.95</sub>Ho<sub>0.05</sub>Sb

The magnetization values of the doped compounds are smaller than that of parent sample and decrease with increasing holmium content. This suggests that the Ho magnetic moments are antiparallely oriented to the transition metals ones, the doped compounds being ferrimagnetically ordered. Therefore, the magnetization measurements are in agreement with results obtained from structural and XPS analysis and confirm that holmium occupies lattice sites. Considering that the magnetic moments per atom of Ni, Mn, Ho and Sb are the same as those calculated in the Ni<sub>8</sub>Mn<sub>7</sub>HoSb<sub>8</sub> compound we have estimated the magnetic moments for the doped compounds. The calculated magnetic moments are  $3.60 \mu_B/\text{f.u.}$  (antiferromagnetic coupling), respectively  $4.01 \mu_B/\text{f.u.}$  (ferromagnetic coupling) for the sample with  $x = 0.05$ . There is a very good agreement between the calculated values in case of antiferromagnetic coupling and experimental values. In all substituted samples similar tendencies was revealed, but the most visible results was observed in case of Ho substitution.

## **D.5 Conclusions on the physical properties of half – Heusler alloy**

- NiMn<sub>1-x</sub>RE<sub>x</sub>Si (with  $x$  between 0 and 0.1 and RE = Gd, Dy, Ho, and Er) compounds were prepared by arc melting the constituent elements in a purified argon atmosphere.
- XRD studies confirm that the prepared samples crystallize in the cubic structure of  $C1b$  type with space group  $F\bar{4}3m$ . In the substituted samples, the structure was unchanged for rare earth concentrations in the range of  $0 < x < 0.05$ . For higher RE concentration a secondary phase appeared.
- TEM investigations are in a good agreement with XRD results. The studied samples were homogeneous and only small inclusion was detected, which do not influence the physical properties of the samples.
- XPS core level and valence band spectra revealed that the doping RE atoms enter in the lattice of the half – Heusler structure. For all the investigated samples, the Mn 3s core – level photoemission spectra show an exchange splitting between 4.5 eV and 5 eV, indicating a strong exchange interaction between the 3s and 3d electrons.
- From DOS calculations the  $f$ - $d$  coupling constant was estimated for all investigated alloys as the  $E_{\text{Ferro}} - E_{\text{Antiferro}}$  energy corresponding to a RE ( $4f$ ) – Mn ( $3d$ ) pair for  $U=8$  eV,  $J=0.9$  eV and for  $U=12$  eV,  $J=0.9$  eV in the case of Ho and respectively Gd doped samples. The minimum energy was found in the case of an antiparallel coupling between Mn ( $3d$ ) and RE ( $4f$ ) spins as expected for heavy rare – earths – 3d transition metals compounds.
- The magnetic moments obtained from magnetization measurements are in very good agreement with the calculated values obtained for an antiparallel orientation of rare earth and transition metals moments.
- The magnetic measurements show decrease of the Curie temperature when Mn atoms are partially substituted by RE in NiMnSb. This is due to the presence of RE ions which influences the strength of the intra Mn( $3d - 3d$ ) sublattice interaction as well as the Ni – Mn interactions.

## Conclusions

- The structural, electronic and magnetic studies of the investigated Heusler and half – Heusler alloys indicate that the the substitution of the Mn with rare earth elements was successful and new materials with possible application in spintronics were synthesized.
- Structural investigations using XRD or TEM revealed that in all investigated samples, if the concentration of the dopant was below 0.05 then a single phase was formed, with the exception is the Tb dopant when only a small amount ( $x = 0.01$ ) of Tb can substitute the Mn and form single phase in all full – and half – Heusler alloys.
- XPS investigations revealed that in all studied samples the RE enters in the structure of the substituted full – and half – Heusler alloys. Also preferentially occupied atomic positions was revealed.
- DOS theoretical computations confirm that, in spite of the substitution, the half – metallicity of the substituted samples is preserved. A good agreement was found between the computed properties and the measured ones.
- The preferential AF coupling between Mn ( $3d$ ) and RE ( $4f$ ) spins, in correlation with DOS results, was revealed in case of all studied half – metallic compounds. Because of the influence on the strength of the intra Mn( $3d - 3d$ ) interaction as well as Ni – Mn interactions, the Curie temperature decreased as it was expected.

## Selected references

- [Borc] C.N. Borca et al., Phys.Rev.B 64, 052409 (2001)
- [Bur] E. Burzo, A. Chelkowski, H.R. Kirchmayr, *Landolt Börnstein Handbook*, Vol. 19d2, Springer – Verlag, Heidelberg 1990, p. 130.
- [Bur2] E. Burzo, I. Balazs, L. Chioncel, E. Arrigoni, F. Beiușeanu, Phys. Rev. B **80**, 214422 (2009)
- [Casp] Casper F, Felser C. Z Allgem Anorg Chem 2008;634:2418 – 22.
- [Cry] Cryogenic, [www.cryogenic.com](http://www.cryogenic.com)
- [Fang] Fang CM, de Wjjs GA, de Groot RA. J Appl Phys 2002;91:8340 – 4
- [Gal1] I. Galanakis, P. H. Dederichs, N. Papanikolaou, Phys. Rev. B 66, 134428 (2002).
- [Gofr] Gofryk K, Kaczorowski D, Plackowski T, Leithe – Jasper A, Grin Y. Phys Rev B 2005;72:094409.
- [Goni] A.Gonis, Green Function for Ordered and Disordered Systems, North – Holland, Amsterdam, 1992.
- [Graf] T. Graf, C. Felser, S. S.P. Parkin, Progress in Solid State Chemistry 39 (2011) 1 – 50
- [Groo] de Groot RA, Mueller FM, van Engen PG, Buschow KHJ. Phys Rev Lett 1983;50:2024.
- [Hart] Hartjes K, Jeitschko W. J Alloys Compd 1995;226:81 – 6.
- [Heyn] Heyne L, Igarashi T, Kanomata T, Neumann K – U, Ouladdiaf B, Ziebeck KRA. J Phys Condens Matter 2005;17:4991 – 9.
- [Ishi4] S. Ishida, S. Asano, and J. Ishida, J. Phys. Soc. Japan. 53 2718 (1984).
- [Itoh] H. Itoh, T. Nakamichi, Y. Yamaguchi, and N. Kazama, Trans. Japan Inst. Met. 24 265 (1983).
- [Ji] Y. Ji, G.J. Strijkers, F.Y. Yang, C.L. Chien, Phys. Rev. B 64 (2001) 224425.
- [Kübl] Kübler J, Williams AR, Sommers CB. Phys Rev B 1983;28:1745 – 55
- [Pacu] R.Pacurariu, PhD thesis, UBB Cluj – Napoca, 2008
- [Paul] Pauling L. Phys Rev 1938;54:899.
- [Slat] Slater JC. Phys Rev 1936;49:537.
- [Stra] P. Strange, Relativistic Quantum Mechanics, University Press, Cambridge, 1998.
- [Tete] R. Tetean, L. Chioncel, E. Burzo, N. Bucur, A Bezerghceanu and I. G. Deac, Applied Surface Science, Vol 255, Issue 3, 685 – 687 (2008)
- [Web] P.J.Webster, J. Phys. Chem. Solids 32 (1971) 1221.
- [Wein] P. Weinberger, Electron Scattering Theory for Order and Disordered Matter, University Press, Oxford, 1990.